

The Antidiabetic Drug Metformin Inhibits Gastric Cancer Cell Proliferation *In Vitro* and *In Vivo*

Kiyohito Kato¹, Jian Gong¹, Hisakazu Iwama⁵, Akira Kitanaka², Joji Tani¹, Hisaaki Miyoshi¹, Kei Nomura¹, Shima Mimura¹, Mitsuyoshi Kobayashi¹, Yuuichi Aritomo¹, Hideyuki Kobara¹, Hirohito Mori¹, Takashi Himoto³, Keiichi Okano⁴, Yasuyuki Suzuki⁴, Koji Murao², and Tsutomu Masaki¹

Abstract

Recent studies suggest that metformin, which is commonly used as an oral anti-hyperglycemic agent of the biguanide family, may reduce cancer risk and improve prognosis, but the mechanisms by which metformin affects various cancers, including gastric cancer, remains unknown. The goal of the present study was to evaluate the effects of metformin on human gastric cancer cell proliferation *in vitro* and *in vivo* and to study microRNAs (miRNA) associated with antitumor effect of metformin. We used MKN1, MKN45, and MKN74 human gastric cancer cell lines to study the effects of metformin on human gastric cancer cells. Athymic nude mice bearing xenograft tumors were treated with or without metformin. Tumor growth was recorded after 4 weeks, and the expression of cell-cycle-related proteins was determined. In addition, we used miRNA array tips to explore the differences among miRNAs in MKN74 cells bearing xenograft tumors treated with or without metformin *in vitro* and *in vivo*. Metformin inhibited the proliferation of MKN1, MKN45, and MKN74 *in vitro*. Metformin blocked the cell cycle in G₀-G₁ *in vitro* and *in vivo*. This blockade was accompanied by a strong decrease of G₁ cyclins, especially in cyclin D1, cyclin-dependent kinase (Cdk) 4, Cdk6 and by a decrease in retinoblastoma protein (Rb) phosphorylation. In addition, metformin reduced the phosphorylation of epidermal growth factor receptor and insulin-like growth factor-1 receptor *in vitro* and *in vivo*. The miRNA expression was markedly altered with the treatment of metformin *in vitro* and *in vivo*. Various miRNAs altered by metformin also may contribute to tumor growth *in vitro* and *in vivo*. *Mol Cancer Ther*; 11(3);549–60. ©2012 AACR.

Introduction

Gastric cancer is now the second-leading cause of cancer-related mortality worldwide, and the prognosis of advanced gastric cancer is poor (1). Apart from potentially curative surgery, chemotherapy and radiochemotherapy may be applied at advanced stages of gastric cancer but neither of these can be curative (2). Thus, there is a strong demand for new curative approaches to advanced gastric cancer.

Metformin is an oral biguanide drug introduced into clinical practice in the 1950s for the treatment of type 2 diabetes (3). It lowers hyperglycemia by inhibiting hepatic glucose production. According to a recent epidemiologic

survey, metformin has significant effects on tumorigenesis. For instance, it is reported that patients with type 2 diabetes who are prescribed metformin have a lower risk of pancreatic cancer than patients who do not take metformin (4). In the basic investigations, metformin inhibited the proliferation of various human cancer cell types, such as those of prostate (5), breast (6), colon (7) and glioma (8). Metformin also inhibited tumor growth in prostate cancer (5) and breast cancer (9) in a mouse xenograft model. Furthermore, in a cancer animal model, metformin treatment decreased the incidence and size of mammary adenocarcinomas in Her2/Neu mice and prevented carcinogen-induced pancreatic cancer in hamsters (10). However, the mechanism underlying the suppression of cancer growth by metformin remains relatively unknown.

Here, we have shown that metformin inhibits the growth of gastric cancer by reducing cyclin D1, cyclin-dependent kinase (Cdk) 4, Cdk 6. In addition, we have identified microRNAs (miRNA) associated with the anti-tumor effect of metformin.

Materials and Methods

Chemicals

Metformin (1,1-dimethylbiguanide monohydrochloride) was purchased from Dainippon Sumitomo Pharma.

Authors' Affiliations: Departments of ¹Gastroenterology and Neurology, ²Laboratory Medicine, ³Integrated Medicine, and ⁴Gastroenterological Surgery, and ⁵Life Science Research Center, Kagawa University School of Medicine, Kagawa, Japan

Note: Supplementary data for this article are available at Molecular Cancer Therapeutics Online (<http://mct.aacrjournals.org/>).

Corresponding Author: Kiyohito Kato, Kagawa University School of Medicine, 1750-1 Ikenobe, Miki-cho, Kita-gun, Kagawa 761-0793, Japan. Phone: 81-087-891-2156; Fax: 81-087-891-2158; E-mail: kato-k@med.kagawa-u.ac.jp

doi: 10.1158/1535-7163.MCT-11-0594

©2012 American Association for Cancer Research.

A Cell Counting Kit (CCK-8) was purchased from Dojindo Laboratories, and all other chemicals were obtained from Sigma Chemical.

Antibodies

In this study, the following antibodies were used: anti- β -actin monoclonal antibody (Sigma-Aldrich; A5441, used at 1:3,000), cyclin D1 (Thermo Fisher Scientific; RB-9041, used at 1:1,000), cyclin E (BD Biosciences; used at 1:1,000), Cdk6 (Santa Cruz Biotechnology; sc-177, used at 1:1,000), Cdk4 (Cell Signaling Technology; #2906, used at 1:1,000), Cdk2 (Santa Cruz Biotechnology; sc-163, used at 1:2,000), phosphorylated retinoblastoma (Rb; BD Pharmingen; 558385, used at 1:1,000), Rb (Cell Signaling Technology; #9309, used at 1:1,000), and secondary horseradish peroxidase (HRP)-linked antimouse and antirabbit IgG antibodies (GE Healthcare UK; used at 1:2,000).

Cell lines and culture

The human gastric cancer cell lines MKN1, MKN45, and MKN74 were obtained from the Japanese Cancer Research Resources Bank and passaged in our laboratory for fewer than 6 months. The cell lines were authenticated by the cell bank using short tandem repeat PCR. Cells were grown in RPMI-1640 (Gibco Invitrogen) supplemented with 10% FBS (533-69545; Wako), and penicillin-streptomycin (100 mg/L; Invitrogen) in a humidified atmosphere of 5% CO₂ at 37°C.

Cell proliferation assay

Cell proliferation assays were conducted using the CCK-8 according to the manufacturer's instructions. Each cell line (1×10^4) was seeded into a well of a 96-well plate and cultured in 100 μ L of RPMI-1640 supplemented with 10% FBS. After 24 hours, seeding cells were treated with 1, 5, and 10 mmol/L metformin and without metformin into the culture medium. At the indicated time points, the medium was exchanged for 110 μ L of RPMI-1640 with CCK-8 reagent (10 μ L CCK-8 and 100 μ L RPMI-1640), and the cells were incubated for 2 hours. Absorbance was measured for each well at a wavelength of 450 nm using an auto-microplate reader.

Cell lysate and tissue lysate

The lysate was conducted according to the methods described in our previous reports (11). All steps were carried out at 4°C. Protein concentration was measured using a dye-binding protein assay based on the Bradford method (12).

Gel electrophoresis and Western blotting

Samples were electrophoresed using 7.5% to 10% SDS-PAGE (13), and the proteins were transferred to nitrocellulose membranes. The membranes were incubated with primary antibodies after blocking and then were incubated with HRP-conjugated secondary antibodies

(14). Immunoreactive proteins were visualized with an enhanced chemiluminescence detection system (Perkin Elmer Co.) on X-ray film.

Flow cytometric analysis

To evaluate the mechanism of growth inhibition by metformin, the cell-cycle profile was analyzed after treatment with metformin. MKN74 cells (1.0×10^6 cells in a 6-well plate dish) were treated with 10 mmol/L metformin or without metformin for 24 to 72 hours. After treatment, the cells were harvested and fixed in 80% ethanol. The fixed cells were washed with PBS and then stored at -20°C until flow cytometric analysis was conducted. On the day of analysis, cells were washed and centrifuged using cold PBS, suspended in 100 μ L PBS and 10 μ L RNase A solution (250 μ g/mL) followed by incubation for 30 minutes at 37°C. Then, 110 μ L propidium iodide (PI) stain (100 μ g/ml) was added to each tube, which was then incubated at 4°C for at least 30 minutes prior to analysis. Flow cytometric analysis was conducted using a Cytomics FC 500 flow cytometer (Beckman Coulter) appointed with an argon laser (488 nm). The percentages of cells in different phases of the cell cycle were analyzed by using FlowJo software (Tree Star). All experiments were carried out in triplicate to assess for consistency of response.

Xenograft model analysis

Animal experiments were carried out according to the guidelines of the Committee on Experimental Animals of Kagawa University, Kagawa, Japan. We purchased 30 male athymic mice (BALB/*c-nu/nu*; 8 weeks old; 20–25 g) from Japan SLC Inc. The animals were maintained under specific pathogen-free conditions using a laminar airflow rack and had continuous free access to sterilized food (γ -ray-irradiated food, CL-2; CLEA Japan Inc.) and autoclaved water. Each mouse was inoculated with MKN74 cells (5×10^6 cells per animal) subcutaneously on the flank regions of the mouse. Two weeks later, the xenografts were identifiable as a mass of more than 6 mm in maximal diameter in all recipients. The animals were randomly assigned to 3 groups. These groups were treated with 1 mg metformin, 2 mg metformin, or control (PBS only), respectively.

The metformin-treated group was injected 5 times a week intraperitoneally (i.p.) at 1 mg/body or 2 mg/body per day for 4 weeks. Only PBS was administered to the control group ($n = 10$) for 4 weeks. After the initiation of the metformin administration, the tumor growth was monitored by the same investigators (K. Kato and T. Masaki), and the tumorigenesis of gastric cancer was monitored every day. Tumor size was measured weekly by measuring the 2 greatest perpendicular tumor dimensions. To examine the significance of the differences between growth curves in this study, all the measurements of tumor volume for each growth curve from the start of the treatment to the end, typically about 30 observations, were analyzed by one-way ANOVA. Tumor volume was calculated as follows: tumor volume (mm³)

= [tumor length (mm) × tumor width (mm)²]/2 (15). All animals were sacrificed on day 28 after treatment. All animals were alive during the observation.

Antibody arrays of phosphorylated receptor tyrosine kinase

RayBio Human Phospho Array Kit (catalog no. ARY 001) was purchased from RayBiotech, Inc. An assay for phosphorylated receptor tyrosine kinase (p-RTK) array was conducted according to the manufacturer's instructions. Briefly, p-RTK array membranes were blocked with 5% bovine serum albumin (BSA)/TBS (0.01 mol/L Tris-HCl, pH 7.6) for 1 hour. The membranes were then incubated with 2 mL of lysate prepared from cell lines or tumorous tissues after normalization with equal amounts of protein. After extensive washing with TBS including 0.1% v/v Tween-20, 3 times for 10 minutes each, and TBS alone, twice for 10 minutes each, to remove unbound materials, the membranes were then incubated with anti-phospho-tyrosine-HRP antibody for 2 hours at room temperature. The unbound HRP antibody was washed out with TBS including 0.1% Tween-20. Finally, each array membrane was exposed to X-ray film using a chemiluminescence detection system (Perkin Elmer Co.). The density of the immunoreactive band obtained on the p-RTK array was analyzed by densitometric scanning (Tlc scanner, Shimizu Co., Ltd.).

Analysis of miRNA microarray

The samples of tumor and cancer cell lines were processed for total RNA extraction with the miRNeasy Mini Kit (Qiagen) according to the manufacturer's instructions. RNA samples typically showed A_{260}/A_{280} ratios of between 1.9 and 2.1, using an Agilent 2100 Bioanalyzer (Agilent Technologies).

After RNA measurement with an RNA 6000 Nano kit (Agilent Technologies), the samples were labeled using a miRCURY Hy3/Hy5 Power Labeling Kit and were hybridized on a human miRNA Oligo chip (v.14.0; Toray Industries). Scanning was conducted with the 3D-Gene Scanner 3000 (Toray Industries). 3D-Gene extraction version 1.2 software (Toray Industries) was used to read the raw intensity of the image. To determine the change in miRNA expression between metformin-treated and control samples, the raw data were analyzed via GeneSpringGX v 10.0 (Agilent Technologies). Samples were first normalized relative to 28sRNA and baseline corrected to the median of all samples.

Replicate data were consolidated into 2 groups: those from metformin-treated animals and those from control animals and were organized by using the hierarchical clustering and ANOVA functions in the GeneSpring software. Hierarchical clustering was done by the use of the clustering function (condition tree) and Euclidean correlation as a distance metric. Two-way ANOVA analysis and asymptotic *P* value computation without any error correction on the samples were conducted to search for the miRNAs that varied most prominently across the differ-

ent groups. The *P* value cutoff was set to 0.05. Only changes >50% for at least one of the time points for each sample were considered significant. All the analyzed data were scaled by global normalization. The statistical significance of differentially expressed miRNAs was analyzed by Student *t* test.

Statistical analysis

All analyses were conducted using the computer-assisted JMP8.0 (SAS Institute). Paired analysis between the groups was conducted using the *t* test. A *P* value of 0.05 was considered to indicate a significant difference between groups.

Results

Metformin inhibits the proliferation of human gastric cancer cell growth

To evaluate the effect of the growth activity of metformin on human gastric cancer cells *in vitro*, we examined the effect of metformin on proliferation in 3 gastric cancer cell lines, MKN1, MKN45, and MKN74. Cells were grown in 10% FBS and treated with 1, 5, and 10 mmol/L metformin or, as a control, without metformin. The cell proliferation assay was conducted 3 days after the addition of the agents. As shown in Fig. 1A, metformin led to a dose-dependent and strong inhibition of cell proliferation in all gastric cancer cell lines, with 49%, 35%, and 51% decreases in the viability of MKN1, MKN45, and MKN74 cells, respectively, with 10 mmol/L metformin.

To discern the direct relationship between the decrease in cell viability and the inhibition of cell proliferation, we followed the course of proliferation over 3 days after the addition of metformin. Metformin (0, 1, 5, and 10 mmol/L) led to a decrease in cell proliferation in a dose- and time-dependent manner in all 3 cell lines tested (Fig. 1B). Together, the results show that metformin inhibits gastric cancer proliferation.

Effects of metformin on cell-cycle-regulatory proteins in MKN74

To study whether or not metformin affects the MKN74 cell cycle, Western blotting was used to examine the expression of various cell-cycle-related molecules in MKN74 with and without metformin treatment. Cells were treated with 10 mmol/L metformin or without metformin for 24 to 72 hours. The most remarkable change was the loss of cyclin D1, a key protein implicated in the transition of the G_0 - G_1 phase. In short, the cyclin D1 level declined slightly at 24 hours after the addition of metformin and was no longer detectable at 48 and 72 hours (Fig. 2A). The level of phosphorylated Rb also decreased progressively in metformin-treated cells. As shown in Fig. 2A, we then studied the expression of other cell-cycle-related proteins (Cdk4, Cdk6, cyclin E, and Cdk2) implicated in the G_0 - G_1 transition. Although Cdk6, the catalytic subunit of cyclin D1, was decreased at 48 and 72 hours after the addition of metformin, Cdk4 was slightly

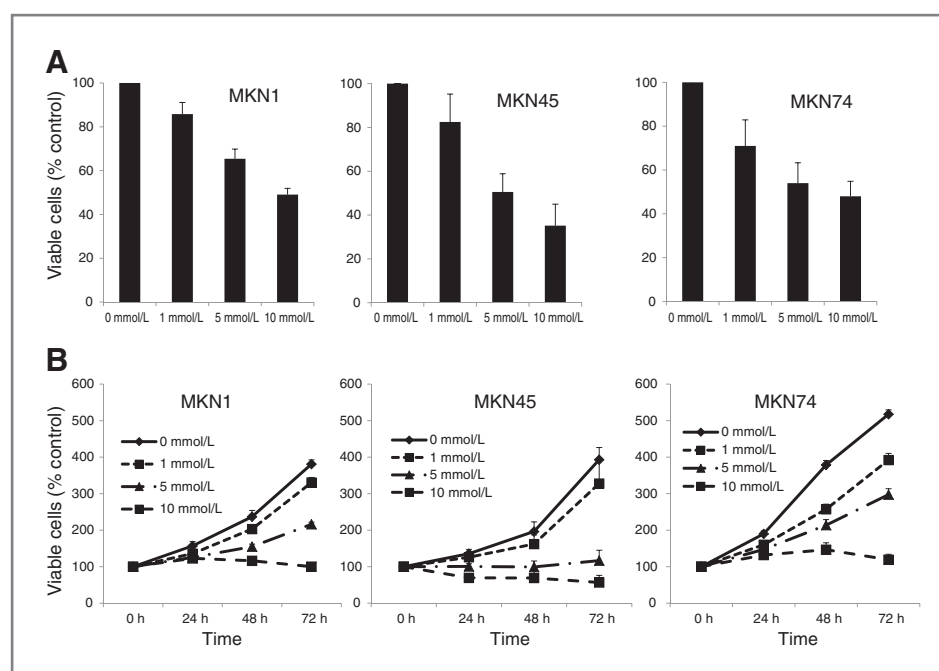


Figure 1. A, metformin inhibits the proliferation of cultured gastric cancer cells. MKN1, MKN45, and MKN74 were seeded in 96-well plates. After 24 hours, metformin (1, 5, and 10 mmol/L) was added to the culture medium. Two days after the addition of the agents, a CCK assay was conducted as described in Materials and Methods. The results are expressed as percentages of viable cells compared with control (0 mmol/L). The mean cell number from 3 independent cultures is shown. Error bars represent SD. Using Student *t* test, all treatments were significantly different from the control ($P < 0.05$). B, MKN1, MKN45, and MKN74 cells were seeded at 10,000 cells per well in a 96-well plate and the agents were added at time 0 hour. A viability assay was conducted daily from time 0 to 72 hours. The data points represent the mean cell number from 3 independent cultures, and the error bars represent SDs. For each cell line, the conditions at 48 and 72 hours are significantly different compared with the control (0 mmol/L), with $P < 0.05$.

decreased at 48 and 72 hours later. Cyclin E was unchanged at 24 hours after metformin treatment but was decreased at 48 and 72 hours after. The catalytic subunit of cyclin E, Cdk2, was also slightly decreased at 48 and 72 hours after the addition of metformin. The level of phosphorylated Rb also decreased progressively in metformin-treated cells. On the other hand, total Rb was the same in cell line irrespective of metformin treatment. These events were detected in other cancer cell lines, such as MKN1 and MKN45 (data not shown).

Next, to further investigate the inhibition of MKN74 cell proliferation in the presence of metformin, the cell-cycle progression was examined by flow cytometry. We treated proliferating MKN74 cells with 10 mmol/L metformin for different durations. After the addition of 10 mmol/L metformin, an increasing number of cells started to accumulate in G_0 - G_1 , 63.0% after 48 hours and 63.5% by 72 hours (Fig. 2B). In parallel, after the addition of 10 mmol/L metformin, we observed reductions in the percentage of cells in the S-phase and G_2 -M phase (Fig. 2B). These data suggest that metformin inhibits cell-cycle progression from G_0 - G_1 into S-phase, resulting in G_1 cell-cycle arrest.

Metformin inhibits tumor proliferation *in vivo*

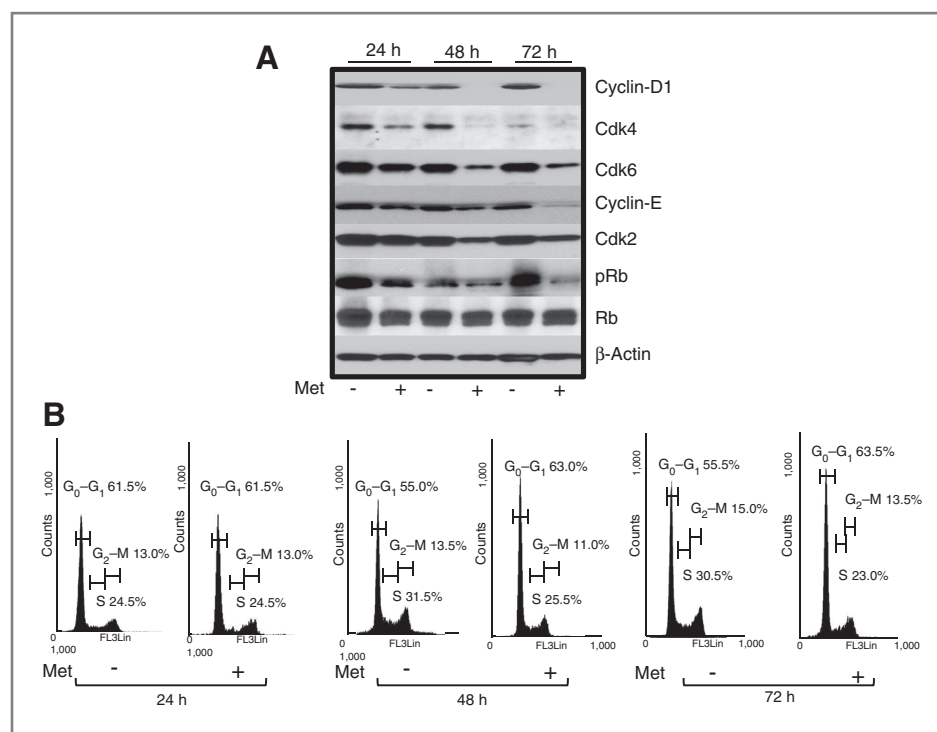
To determine whether or not metformin could affect tumor growth *in vivo*, we injected nude mice subcutane-

ously with MKN74 cells. Metformin was injected daily intraperitoneally at 1 or 2 mg.

On the basis of the integrated values of the tumor growth curves, intraperitoneal administration of metformin led to the substantial inhibition of tumor growth, by 41% (1 mg/d) and 78% (2 mg/d; Fig. 3A and B, $P = 0.0207$, one-way ANOVA). These growth rates were significantly above those of the control ($P < 0.01$ and $P < 0.004$, respectively). In addition, 2 mg metformin treatment significantly inhibited tumor growth compared with 1 mg metformin-treated mice ($P < 0.007$). In this study, metformin exhibited no apparent changes in mice and did not affect their weight (data not shown). All animals were alive during the experiment.

To determine whether or not metformin also affects cell-cycle-regulatory protein levels *in vivo*, we analyzed protein expression using Western blotting in tumors obtained from the xenograft experiments. Metformin reduced significantly the levels of these proteins (phosphorylated Rb, cyclin D1, Cdk2, Cdk4, Cdk6, and cyclin E) in treated tumors compared with controls (Fig. 3C). On the other hand, total Rb was the same in cell line irrespective of metformin. These results suggest that, similar to the results of the *in vitro* observations (Fig. 2A), metformin decreases tumor growth by reducing cell-cycle-regulatory protein levels, resulting in G_1 cell-cycle arrest.

Figure 2. Metformin blocks the cell cycle in G₀-G₁ and affects the expression levels of the various cell-cycle-regulatory proteins in MKN74 cells. A, Western blotting of cyclin D1, Cdk4, Cdk6, cyclin E, Cdk2, phosphorylated Rb (pRb), and Rb in MKN74 cells of 24, 48, and 72 hours after the addition of 10 mmol/L metformin (Met) for the indicated time. B, flow cytometric analysis of proliferating MKN74 cells 24, 48, and 72 hours after the addition of 10 mmol/L metformin (Met). Results are representative of 3 independent experiments.



Differences in p-RTKs *in vitro* and *in vivo* treated with and without metformin

We used a p-RTK array system to identify the "key RTKs" associated with the antitumor effect of metformin. By using the antibody array (Fig. 4A), we simultaneously screened the expressions of 42 different activated RTKs in MKN74 cells and tumors with or without metformin. Metformin reduced the expression of phosphorylated epidermal growth factor receptor (p-EGFR; Fig. 4B and D) and that of phosphorylated insulin-like growth factor-1 receptor (p-IGF-1R; Fig. 4C and D) *in vitro* and *in vivo*, as the protein array detected.

Densitometric data on p-EGFR and p-IGF-1R in cell line and tumorous tissue were expressed as black and white, respectively. The density of the p-EGFR and that of the p-IGF-1R obtained from the membrane array were analyzed by means of an Image Station (Eastman Kodak). The densitometric ratios of the p-EGFR and p-IGF-1R spots of the metformin-treated cell line to nontreated metformin were 68.8% and 4.0%, respectively (Fig. 4D). In addition, the ratios of p-EGFR and p-IGF-1R of metformin-treated tumorous tissue to nontreated metformin were 39.7% and 19.8%, respectively (Fig. 4D).

Differences in miRNA expression in the cell lines *in vitro* and tumorous tissues *in vivo* treated with and without metformin

Using a custom microarray platform, we analyzed the expression levels of 985 human miRNA probes in the cell lines *in vitro* and tumorous tissues *in vivo* that were treated

with and without metformin. As shown Table 1, when the expression of miRNAs was studied in MKN74 cells treated with 10 mmol/L metformin and without metformin *in vitro*, 30 miRNAs were significantly upregulated (Table 1) in MKN74 cells after 72 hours of metformin treatment whereas 21 miRNAs were downregulated (Table 1). In a tumor xenograft model, in the metformin group, there were 22 upregulated (Table 2) and 21 downregulated miRNAs (Table 2) of the 985 miRNAs (GEO, accession no.GSE30289). In Tables 1 and 2, the 7 miRNAs marked with a dagger were matched with ones from both cultured cells and xenograft tissues after metformin treatment.

Unsupervised hierarchical clustering analysis, using Pearson's correlation, showed that cell lines *in vitro* and tumorous tissues *in vivo* treated with metformin clustered together and separately from the untreated cell lines (Fig. 5A) and tissues (Fig. 5B). These subsets of 51 microRNAs in cell lines and 43 miRNAs in tissues were found to exhibit >1.5-fold alterations in expression levels between the metformin-treated and control groups.

Discussion

The incidence and mortality rate of gastric cancer have decreased dramatically over the past several decades. Nonetheless, the disease remains a major public health issue as the second-leading cause of cancer death worldwide (16). Apart from potentially curative surgery, chemotherapy and radiochemotherapy may be applied at advanced stages in gastric cancer but neither can cure the

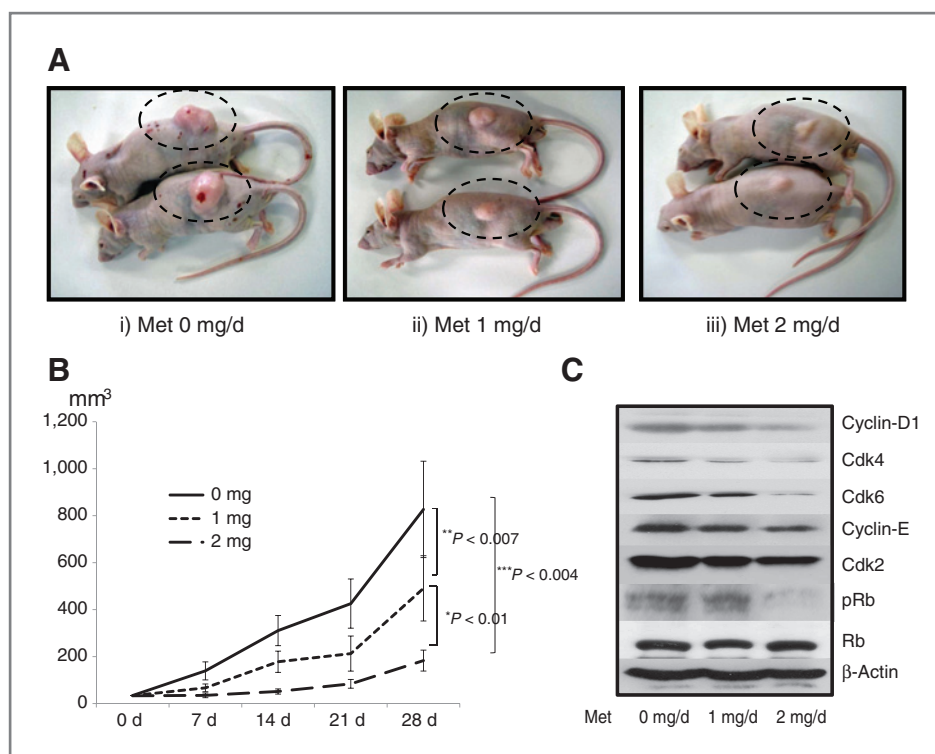


Figure 3. *In vivo* antitumor effects of metformin on established gastric cancer in nude mice. **A**, representative photographs of the gross MKN74 tumors from nude mice treated with control (i), 1 mg metformin (ii), or 2 mg metformin (iii). **B**, MKN74 cells implanted subcutaneously into the flank regions of nude mice. When a tumor became palpable, 1 and 2 mg metformin was injected intraperitoneally for 4 weeks, 5 times per week. Animals in the control group developed rapidly growing subcutaneous gastric cancer. In contrast, animals in the metformin groups exhibited significantly retarded tumor development. The tumors in the mice treated with 2 mg metformin (Met) were significantly smaller than those in the mice treated with 1 mg metformin. Each data point represents the mean \pm SD of 10 animals. $P = 0.0207$, one-way ANOVA; *, $P < 0.01$; **, $P < 0.007$; ***, $P < 0.004$. Tumor volumes (mm³) are expressed as follows: tumor volume (mm³) = [tumor length (mm) \times tumor width (mm)²]/2. **C**, representative Western blotting of cell-cycle-regulatory protein expression in tumors from mice treated with and without metformin (Met). Various cell-cycle-related proteins in the tumorous tissues treated with metformin were reduced as compared with control nude mice.

disease in such cases and the prognosis is poor. Thus, there is strong demand for new curative approaches to gastric cancer therapy.

The role of the antidiabetic drug metformin in glucose and fatty acid metabolism is very well known (17, 18). In mice, at doses of 1 to 3 mg/d, it stimulates glucose uptake and increases fatty acid oxidation in muscle and liver with no side effects (5). Recent data suggest that metformin could protect from cancer and inhibit proliferation in various cancer cell lines, such as breast (11), glial (9), and prostate cancer (5). However, the antitumor effect of metformin for gastric cancer remains unknown. Here, we show that metformin not only is a very potent inhibitor of human gastric cancer cell growth but also inhibits tumorigenesis in a xenograft model when administered intraperitoneally.

Specific cyclin/Cdk complexes are activated at different intervals during the cell cycle. Complexes of Cdk4 and Cdk6 with cyclin D1 are required for G₁ phase progression, whereas complexes of Cdk2 with cyclin E are required for the G₁-S transition (19). In previous reports, downregulation of cyclin D1 in response to metformin has been shown in various cancer cell lines, such as colon (7),

breast (20), and prostate cancer (5). However, the effects of metformin on catalytic subunits of cyclin D1, Cdk4 and Cdk6, remain unknown. In the present study, the major cell-cycle regulators (cyclin D1, Cdk4, Cdk6, cyclin E, Cdk2, phosphorylated Rb) could be intracellular targets of the metformin-mediated antiproliferative effect in human gastric cancers *in vitro*. In addition, flow cytometry revealed that metformin arrested gastric cancer cells at the G₀-G₁ phase *in vitro*. A subsequent *in vitro* experiment using subcutaneous gastric cancer-bearing athymic nude mice also showed that metformin markedly suppressed the growth of gastric cancer, and the expression levels of numerous cell-cycle molecules (cyclin D1, Cdk4, Cdk6, cyclin E, Cdk2, phosphorylated Rb) were found to be reduced by treatment with metformin, indicating that metformin may inhibit the expression of cell-cycle-related molecules, especially in cyclin D1 in MKN74 cells *in vivo*. These data suggest that the antitumor effect of metformin may be related to the reduction of various cell-cycle-related proteins, especially in cyclin D1.

Our *in vitro* study was conducted using a higher dose of metformin than the human therapeutic concentration (6–30 μ mol/L). The use of such higher doses has been the

Table 1. Statistical results and chromosomal locations of miRNAs in MKN74 cells treated with metformin, compared with nontreated cells

miRNA	Fold (treated/nontreated), mean \pm SD	P	Chromosomal localization
Upregulated			
hsa-miR-638	3.31 \pm 1.05	0.0083	19p13.2
hsa-miR-1246	2.65 \pm 1.12	0.0036	2q31.1
hsa-miR-1228*	2.59 \pm 1.56	0.0145	12
hsa-miR-1469	2.55 \pm 1.73	0.029	15q26.2
hsa-miR-762	2.30 \pm 0.25	0.0008	16
hsa-miR-1268	2.24 \pm 0.96	0.0248	15q11.2
hsa-miR-1908	2.04 \pm 0.87	0.0081	11
hsa-miR-663	2.04 \pm 0.72	0.0133	20p 11.1
hsa-miR-423-3p	2.01 \pm 0.84	0.0186	17q11.2
hsa-miR-31	1.79 \pm 0.99	0.0367	9p21.3
hsa-let-7b	1.67 \pm 1.02	0.0024	22q13.31
hsa-miR-1973	1.63 \pm 0.70	0.0106	4
hsa-miR-934	1.58 \pm 0.53	0.0349	Xq26.3
hsa-miR-27b	1.53 \pm 0.56	0.0204	9q22.32
hsa-miR-182	1.52 \pm 0.45	0.0173	7q32.2
hsa-miR-1977	1.51 \pm 0.35	0.0003	1
hsa-miR-149	1.48 \pm 0.46	0.0026	2q37.3
hsa-miR-125a-5p	1.48 \pm 0.81	0.0353	19q13.41
hsa-miR-27a	1.47 \pm 0.42	0.0016	19p13.13
hsa-miR-361-5p ^a	1.47 \pm 0.61	0.0477	X
hsa-miR-200a	1.41 \pm 0.33	0.0144	1p36.33
hsa-miR-26b ^a	1.40 \pm 0.29	0.0039	2q35
hsa-miR-22	1.39 \pm 0.29	0.0018	17p13.3
hsa-miR-24	1.35 \pm 0.40	0.003	9q22.32
hsa-let-7c	1.28 \pm 0.26	0.041	21q21.1
hsa-miR-21 ^a	1.27 \pm 0.17	0.0034	17q23.1
hsa-miR-18a	1.25 \pm 0.43	0.048	13q31.3
hsa-miR-200c	1.23 \pm 0.12	0.0012	12p13.31
hsa-let-7f ^a	1.17 \pm 0.12	0.0047	9q22.32
hsa-miR-1975	1.16 \pm 0.21	0.0341	7
Downregulated			
hsa-miR-1826 ^a	0.520 \pm 0.166	0.0147	16
hsa-miR-1979	0.621 \pm 0.100	0.0002	4q32.3
hsa-miR-1260 ^a	0.630 \pm 0.121	0.0009	14
hsa-miR-30e*	0.679 \pm 0.229	0.0182	1p34.2
hsa-miR-182*	0.682 \pm 0.274	0.0045	7q32.2
hsa-miR-422a	0.691 \pm 0.245	0.0255	15q22.31
hsa-miR-372	0.692 \pm 0.226	0.0026	19q13.42
hsa-miR-1280 ^a	0.703 \pm 0.197	0.0171	3
hsa-miR-130b	0.708 \pm 0.325	0.01	22
hsa-miR-18b	0.716 \pm 0.290	0.0086	Xq26.2
hsa-miR-221	0.719 \pm 0.224	0.0111	Xp11.3
hsa-miR-320b	0.734 \pm 0.215	0.014	1
hsa-miR-320c	0.738 \pm 0.301	0.0164	18q11.2
hsa-miR-151-3p	0.751 \pm 0.238	0.0178	8
hsa-miR-1274b	0.759 \pm 0.235	0.0316	19
hsa-miR-7	0.771 \pm 0.202	0.0152	9q21.32
hsa-miR-30e	0.774 \pm 0.171	0.02	1p34.2
hsa-miR-24-2*	0.775 \pm 0.253	0.0126	19p13.13
hsa-miR-1274a	0.818 \pm 0.156	0.0302	5p13.1
hsa-miR-720	0.827 \pm 0.196	0.0376	3
hsa-miR-23b	0.858 \pm 0.240	0.0265	9q22.32

^aMiRNAs that were matched to miRNAs extracted from cultured cells and tumorous tissues after treatment with metformin.

Table 2. Statistical results and chromosomal locations of miRNAs in gastric cancer tumors treated with metformin, compared with nontreated cells

miRNA	Fold (treated/nontreated), mean \pm SD	P	Chromosomal localization
Upregulated			
hsa-miR-199a-3p	6.03 \pm 3.23	0.0001	19p 13.2
hsa-miR-21 ^a	4.03 \pm 2.77	0.0082	17q23.1
hsa-miR-223	3.63 \pm 2.23	0.040	Xq12
hsa-miR-342-3p	3.56 \pm 1.80	0.041	14q32.2
hsa-miR-126	3.43 \pm 2.62	0.0068	9q34.3
hsa-miR-146b-5p	3.18 \pm 1.23	0.022	10q24.32
hsa-miR-361-5p ^a	3.13 \pm 1.52	0.018	X
hsa-miR-99a	3.11 \pm 1.53	0.0019	21q21.1
hsa-miR-16	2.31 \pm 1.17	0.0045	13q14.2
hsa-miR-1308	2.10 \pm 0.93	0.0086	Xp22.1
hsa-miR-26b ^a	2.28 \pm 0.97	0.010	2q35
hsa-let-7g	1.98 \pm 0.90	0.040	3p21.1
hsa-let-7e	1.97 \pm 1.36	0.004	19q13.41
hsa-miR-191	1.97 \pm 0.49	0.008	3p21.31
hsa-let-7f ^a	1.90 \pm 0.85	0.002	9q22.32
hsa-miR-26a	1.80 \pm 0.73	0.025	3p22.2
hsa-miR-425	1.67 \pm 0.34	0.0008	3p21.31
hsa-miR-18a	1.56 \pm 0.51	0.030	13q31.3
hsa-miR-25	1.47 \pm 0.57	0.037	7q22.1
hsa-miR-483-3p	1.43 \pm 0.13	0.003	11p15.5
hsa-miR-106a	1.43 \pm 0.47	0.003	Xq26.2
hsa-miR-934	1.29 \pm 0.17	0.040	Xq26.3
Downregulated			
hsa-miR-1978	0.316 \pm 0.153	0.0048	2
hsa-miR-711	0.399 \pm 0.338	0.003	3
hsa-miR-874	0.488 \pm 0.176	0.0056	5q31.2
hsa-miR-1973	0.519 \pm 0.205	0.004	4
hsa-miR-532-3p	0.589 \pm 0.437	0.033	Xp11.23
hsa-miR-886-5p	0.603 \pm 0.332	0.006	5q31.1
hsa-miR-760	0.606 \pm 0.371	0.026	1p22.1
hsa-miR-1977	0.609 \pm 0.277	0.0059	1
hsa-miR-1908	0.616 \pm 0.176	0.0002	11
hsa-miR-1826 ^a	0.618 \pm 0.085	0.021	16
hsa-miR-125a-3p	0.643 \pm 0.230	0.0104	19q13.41
hsa-miR-1975	0.649 \pm 0.154	0.0075	7
hsa-miR-1285	0.652 \pm 0.326	0.032	7q21-q22
hsa-miR-494	0.665 \pm 0.141	0.006	14q32.31
hsa-miR-361-3p	0.736 \pm 0.288	0.045	x
hsa-miR-1913	0.751 \pm 0.195	0.014	6
hsa-miR-339-5p	0.765 \pm 0.203	0.018	7p22.3
hsa-miR-92b	0.776 \pm 0.191	0.012	1q22
hsa-miR-1260 ^a	0.812 \pm 0.141	0.028	14
hsa-miR-744	0.828 \pm 0.190	0.045	17p12
hsa-miR-1280 ^a	0.854 \pm 0.177	0.015	3

^aMiRNAs that were matched to miRNAs extracted from cultured cells and tumorous tissues after treatment with metformin.

treatment and to provide clues to the molecular basis of the anti-cancer effects of metformin, particularly when mediated with miRNAs.

We found that members of the let-7 family are upregulated in both cultured cells and tumorous tissues treated with metformin. The human let-7 family

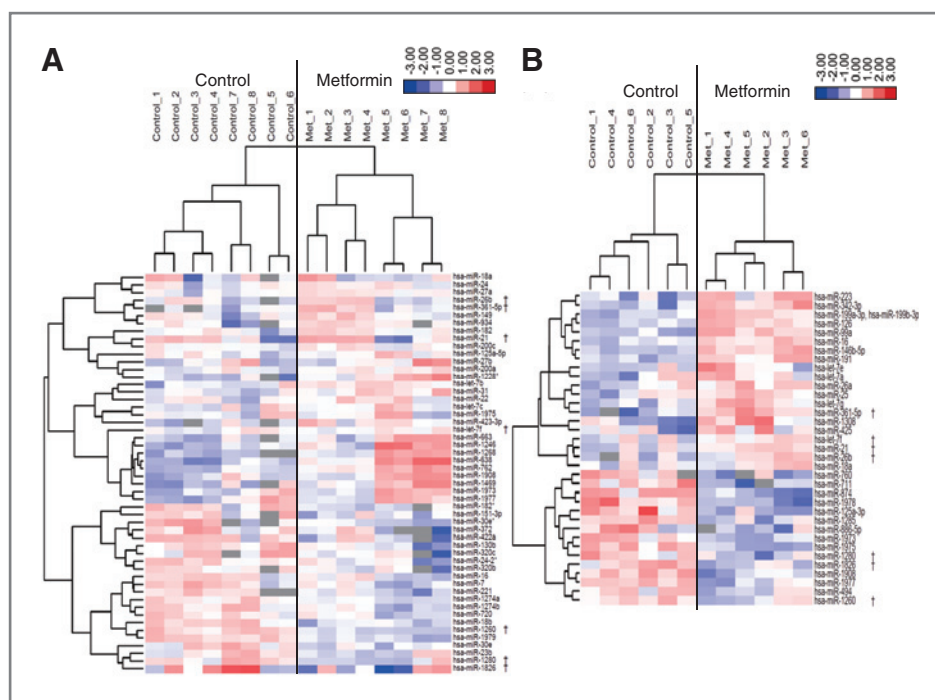


Figure 5. A, hierarchical clustering of MKN74 with and without metformin. MKN74 cells were clustered according to the expression profiles of 51 differently expressed miRNAs between MKN74 cells treated with metformin and those treated without it. B, hierarchical clustering of tumor samples from a xenograft animal model with and without metformin. Tumor tissues were clustered according to the expression profiles of 41 differentially expressed miRNAs between tumorous tissues with metformin treatment and those without it. A and B, the analyzed samples are in columns and the miRNAs are presented in rows. The miRNA clustering tree is shown on the left and the sample clustering tree appears at the top. The color scale shown at the top illustrates the relative expression level of miRNAs; red represents a high expression level, blue represents a low expression level. miRNAs marked with a dagger are matched miRNAs extracted from cultured cells and tumorous tissues after treatment with metformin.

containing 13 members is widely recognized as a class of miRNAs producing a tumor-suppressing effect (31). Consistent with this events, downregulation of let-7 family members has been reported in many cancers, such as lung (32), breast (33), colorectal cancer (34), and melanoma (35). The let-7 family acts as a tumor suppressor by binding its target oncogenes, including the *Ras* (36), *HMG2* (37), *c-Myc* (38), and various cell-cycle regulators. Among upregulated let-7 family members in cell culture in the present study, let-7b overexpression in melanoma cells *in vitro* leads to the downregulation of the expression of cyclins D1, D3 and A, as well as to the downregulation of Cdk 4 (35, 39). In addition, let-7g targets cell-cycle control genes such as *cyclin D1*, *E2F1*, *Ras*, and *c-myc* and restrains the growth of hepatoma cells (40). Thus, our results suggest that metformin-induced inhibition of human gastric cancer cell proliferation is mediated, in part, by the tumor suppressor activities caused by upregulation of let-7 family members.

We also found differentially expressed miRNAs in cultured cells and tumorous tissues treated with metformin as compared with untreated cells. Among upregulated miRNAs in culture cells treated, hsa-mir-663 inhibits the growth of gastric cancer (41), hsa-mir-22 inhibits the growth of hepatocellular carcinoma (42), and hsa-mir-182

inhibits the growth of lung cancer (43). Especially, the expression of hsa-mir-638 in metformin-treated cells was 3.3 times higher than that in untreated cells. The hsa-mir-638 is one of the miRNAs most abundantly expressed in normal serum. Although the physiologic significance of hsa-mir-638 is not adequately known, one report shows decreased expression of hsa-mir-638 in gastric cancer tissues (44). Thus, our data suggest that hsa-mir-638 may be a candidate for a new therapeutic target in gastric cancer.

In the present study, we found only 7 matched miRNAs extracted from cultured cells and tumorous tissues after treatment with metformin. Although many miRNAs were significantly altered after metformin treatment, we found several differences in the profiles of miRNA expression between the cultured cells and tumorous tissues. This discrepancy could reflect the differences between *in vitro* and *in vivo* models. In short, metformin is directly exposed to *in vitro* cultured cells, whereas intraperitoneally administered metformin is metabolized *in vivo*. In addition, tumor cells in mice are affected by the host's immune response. Furthermore, there are differences in exposure times and metformin concentrations between the *in vitro* and *in vivo* models. Therefore, differences in exposure times and concentrations of metformin

may result in the differential expression profiles of miRNAs.

In conclusion, our results revealed that metformin inhibits human gastric cancer cell proliferation and tumor growth, possibly by suppressing the cell-cycle-related molecules via alteration of miRNAs. Metformin postponed spontaneous carcinogenesis in mice and rats, as well as chemical and radiation carcinogenesis in mice, rats, and hamsters (45). In addition, in female SHR mice, metformin increased life span and postponed tumors when started at young or middle age but not when started at old age (46). These data suggest that metformin might be a more effective treatment for young patients with gastric cancer.

Metformin is a drug widely used for the treatment of type 2 diabetes with limited side effects. Therefore, metformin may become a novel and effective therapy for the

treatment and long-term management of gastric cancer, providing additional benefits at low cost.

Supporting information available

Supplementary Data S1. This material is available free of charge via the Internet at <http://www.microna.org> and <http://www.ncbi.nlm.nih.gov/genet>.

Disclosure of Potential Conflicts of Interest

No potential conflicts of interests were disclosed.

The costs of publication of this article were defrayed in part by the payment of page charges. This article must therefore be hereby marked *advertisement* in accordance with 18 U.S.C. Section 1734 solely to indicate this fact.

Received August 3, 2011; revised December 5, 2011; accepted December 19, 2011; published OnlineFirst January 5, 2012.

References

- Smith JK, McPhee JT, Hill JS, Whalen GF, Sullivan ME, Litwin DE, et al. National outcomes after gastric resection for neoplasm. *Arch Surg* 2007;142:387–93.
- Lordick F, Siewert JR. Recent advances in multimodal treatment for gastric cancer: a review. *Gastric Cancer* 2005;8:78–85.
- Witters LA. The blooming of the French lilac. *J Clin Invest* 2001;108:1105–7.
- Lee M-S, Hsu C-C, Wahlqvist ML, Tsai H-N, Chang Y-H, Huang Y-C. Type 2 diabetes increases and metformin reduces total, colorectal, liver and pancreatic cancer incidences in Taiwanese: a representative population prospective cohort study of 800,000 individuals. *BMC Cancer* 2011;11:20.
- Ben Sahara I, Laurent K, Loubat A, Giorgetti-Peraldi S, Colosetti P, Auberger P, et al. The antidiabetic drug metformin exerts an antimetastatic effect *in vitro* and *in vivo* through a decrease of cyclin D1 level. *Oncogene* 2008;27:3576–86.
- Brown KA, Hunger NI, Docanto M, Simpson ER. Metformin inhibits aromatase expression in human breast adipose stromal cells via stimulation of AMP-activated protein kinase. *Breast Cancer Res Treat* 2010;123:591–96.
- Zhou XZ, Xue YM, Zhu B, Sha JP. [Effects of metformin on proliferation of human colon carcinoma cell line SW-480]. *Nan Fang Yi Ke Da Xue Xue Bao* 2010;30:1935–8, 1942.
- Isakovic A, Harhaji L, Stevanovic D, Markovic Z, Sumarac-Dumanovic M, Starcevic V, et al. Dual antiangiogenic action of metformin: cell cycle arrest and mitochondria-dependent apoptosis. *Cell Mol Life Sci* 2007;64:1290–302.
- Anisimov VN, Berstein LM, Egorin PA, Piskunova TS, Popovich IG, Zabezhinski MA, et al. Effect of metformin on life span and on the development of spontaneous mammary tumors in HER-2/neu transgenic mice. *Exp Gerontol* 2005;40:685–93.
- Anisimov VN, Egorin PA, Piskunova TS, Popovich IG, Tyndyk ML, Yurova MN, et al. Metformin extends life span of HER-2/neu transgenic mice and in combination with melatonin inhibits growth of transplantable tumors *in vivo*. *Cell Cycle* 2010;9:188–97.
- Masaki T, Tokuda M, Yoshida S, Nakai S, Morishita A, Uchida N, et al. Comparison study of the expressions of myristoylated alanine-rich C kinase substrate in hepatocellular carcinoma, liver cirrhosis, chronic hepatitis, and normal liver. *Int J Oncol* 2005;26:661–71.
- Bradford MM. A rapid and sensitive method for the quantitation of microgram quantities of protein utilizing the principle of protein-dye binding. *Anal Biochem* 1976;72:248–54.
- Laemmli UK. Cleavage of structural proteins during the assembly of the head of bacteriophage T4. *Nature* 1970;227:680–5.
- Towbin H, Staehelin T, Gordon J. Electrophoretic transfer of proteins from polyacrylamide gels to nitrocellulose sheets: procedure and some applications. *Proc Natl Acad Sci U S A* 1979;76:4350–4.
- D'Incalci M, Colombo T, Ubezio P, Nicoletti I, Giavazzi R, Erba E, et al. The combination of yonidol and cisplatin is synergistic against human tumor xenografts. *Eur J Cancer* 2003;39:1920–6.
- Ohtsu A, Yoshida S, Saijo N. Disparities in gastric cancer chemotherapy between the East and West. *J Clin Oncol* 2006;24:2188–96.
- Correia S, Carvalho C, Santos MS, Seica R, Oliveira CR, Moreira PI. Mechanisms of action of metformin in type 2 diabetes and associated complications: an overview. *Mini Rev Med Chem* 2008;8:1343–54.
- Zhou G, Myers R, Li Y, Chen Y, Shen X, Fenyk-Melody J, et al. Role of AMP-activated protein kinase in mechanism of metformin action. *J Clin Invest* 2001;108:1167–74.
- Masaki T, Shiratori Y, Rengifo W, Igarashi K, Yamagata M, Kurokohchi K, et al. Cyclins and cyclin-dependent kinases: comparative study of hepatocellular carcinoma versus cirrhosis. *Hepatology* 2003;37:534–43.
- Zhuang Y, Miskimins WK. Cell cycle arrest in Metformin treated breast cancer cells involves activation of AMPK, downregulation of cyclin D1, and requires p27Kip1 or p21Cip1. *J Mol Signal* 2008;3:18.
- Liu B, Fan Z, Edgerton SM, Deng XS, Alimova IN, Lind SE, et al. Metformin induces unique biological and molecular responses in triple negative breast cancer cells. *Cell Cycle* 2009;8:2031–40.
- Han S, Kim HY, Park K, Lee MS, Kim HJ, Kim YD. Expression of p27Kip1 and cyclin D1 proteins is inversely correlated and is associated with poor clinical outcome in human gastric cancer. *J Surg Oncol* 1999;71:147–54.
- Aoyagi K, Koufujii K, Yano S, Murakami N, Terasaki Y, Yamasaki Y, et al. Immunohistochemical study on the expression of cyclin D1 and E in gastric cancer. *Kurume Med J* 2000;47:199–203.
- Vazquez-Martin A, Oliveras-Ferreros C, Cufi S, Martin-Castillo B, Menendez JA. Metformin activates an Ataxia Telangiectasia Mutated (ATM)/Chk2-regulated DNA damage-like response. *Cell Cycle* 2011;9:1499–501.
- Wang LW, Li ZS, Zou DW, Jin ZD, Gao J, Xu GM, et al. Metformin induces apoptosis of pancreatic cancer cells. *World J Gastroenterol* 2008;47:7192–8.
- Perry JE, Grossmann ME, Tindall DJ. Epidermal growth factor induces cyclin D1 in a human prostate cancer cell line. *Prostate* 1998;35:117–24.
- Herbst RS, Shin DM. Monoclonal antibodies to target epidermal growth factor receptor-positive tumors: a new paradigm for cancer therapy. *Cancer* 2002;94:1593–611.

28. Ren M, Zhong X, Ma CY, Sun Y, Guan QB, Cui B, et al. Insulin-like growth factor-1 promotes cell cycle progression via upregulation of cyclin D1 expression through the phosphatidylinositol 3-kinase/nuclear factor-kappaB signaling pathway in FRTL thyroid cells. *Acta Pharmacol Sin* 2009;30:113–9.
29. Pollak M. Insulin and insulin-like growth factor signalling in neoplasia. *Nat Rev Cancer* 2008;8:915–28.
30. Rosenthal SM, Cheng ZQ. Opposing early and late effects of insulin-like growth factor I on differentiation and the cell cycle regulatory retinoblastoma protein in skeletal myoblasts. *Proc Natl Acad Sci U S A* 1995;92:10307–11.
31. Boyerinas B, Park SM, Hau A, Murmann AE, Peter ME. The role of let-7 in cell differentiation and cancer. *Endocr Relat Cancer* 2010;17:F19–36.
32. Takamizawa J, Konishi H, Yanagisawa K, Tomida S, Osada H, Endoh H, et al. Reduced expression of the let-7 microRNAs in human lung cancers in association with shortened postoperative survival. *Cancer Res* 2004;64:3753–6.
33. Yu F, Yao H, Zhu P, Zhang X, Pan Q, Gong C, et al. let-7 regulates self renewal and tumorigenicity of breast cancer cells. *Cell* 2007;131:1109–23.
34. Akao Y, Nakagawa Y, Naoe T. let-7 microRNA functions as a potential growth suppressor in human colon cancer cells. *Biol Pharm Bull* 2006;29:903–6.
35. Fu TY, Chang CC, Lin CT, Lai CH, Peng SY, et al. Let-7b-mediated suppression of basigin expression and metastasis in mouse melanoma cells. *Exp Cell Res* 2011;317:445–51.
36. Johnson SM, Grosshans H, Shingara J, Byrom M, Jarvis R, Cheng A, et al. RAS is regulated by the let-7 microRNA family. *Cell* 2005;120:635–47.
37. Lee YS, Dutta A. The tumor suppressor microRNA let-7 represses the HMGA2 oncogene. *Genes Dev* 2007;21:1025–30.
38. Osada H, Takahashi T. let-7 and miR-17-92: small-sized major players in lung cancer development. *Cancer Sci* 2011;102:9–17.
39. Schultz J, Lorenz P, Gross G, Ibrahim S, Kunz M. MicroRNA let-7b targets important cell cycle molecules in malignant melanoma cells and interferes with anchorage-independent growth. *Cell Res* 2008;18:549–57.
40. Lan FF, Wang H, Chen YC, Chan CY, Ng SS, Li K, Xie D, et al. Hsa-let-7g inhibits proliferation of hepatocellular carcinoma cells by down-regulation of c-Myc and upregulation of p16(INK4A). *Int J Cancer* 2011;128:319–31.
41. Pan J, Hu H, Zhou Z, Sun L, Peng L, Yu L, et al. Tumor-suppressive mir-663 gene induces mitotic catastrophe growth arrest in human gastric cancer cells. *Oncol Rep* 2010;24:105–12.
42. Zhang J, Yang Y, Yang T, Liu Y, Li A, Fu S, et al. microRNA-22, downregulated in hepatocellular carcinoma and correlated with prognosis, suppresses cell proliferation and tumorigenicity. *Br J Cancer* 2010;103:1215–20.
43. Sun Y, Fang R, Li C, Li L, Li F, Ye X, et al. Hsa-mir-182 suppresses lung tumorigenesis through down regulation of RGS17 expression *in vitro*. *Biochem Biophys Res Commun* 2010;396:501–7.
44. Tsukamoto Y, Nakada C, Noguchi T, Tanigawa M, Nguyen LT, Uchida T, et al. MicroRNA-375 is downregulated in gastric carcinomas and regulates cell survival by targeting PDK1 and 14-3-3zeta. *Cancer Res* 2010;70:2339–49.
45. Anisimov VN. Metformin for aging and cancer prevention. *Aging (Albany NY)* 2010;11:760–74.
46. Anisimov VN, Berstein LM, Popovich IG, Zabezhinski MA, Egorin PA, Piskunova TS, et al. If started early in life, metformin treatment increase life span and postpones tumors in female SHR mice. *Aging (Albany NY)* 2011;2:148–57.